Mol. Cells *29*, 397-405, April 30, 2010
DOI/10.1007/s10059-010-0047-6

Molecules and Cells

Structural Basis for the Reaction Mechanism of UDP-Glucose Pyrophosphorylase

Hun Kim, Jongkeun Choi, Truc Kim, Neratur K. Lokanath[1], Sung Chul Ha, Se Won Suh[2], Hye-Yeon Hwang, and Kyeong Kyu Kim*

UDP-glucose pyrophosphorylases (UGPase; EC 2.7.7.9) catalyze the conversion of UTP and glucose-1-phosphate to UDP-glucose and pyrophosphate and *vice versa*. Prokaryotic UGPases are distinct from their eukaryotic counterparts and are considered appropriate targets for the development of novel antibacterial agents since their product, UDP-glucose, is indispensable for the biosynthesis of virulence factors such as lipopolysaccharides and capsular polysaccharides. In this study, the crystal structures of UGPase from *Helicobacter pylori* (HpUGPase) were determined in apo- and UDP-glucose/Mg^{2+}-bound forms at 2.9 Å and 2.3 Å resolutions, respectively. HpUGPase is a homotetramer and its active site is located in a deep pocket of each subunit. Magnesium ion is coordinated by Asp130, two oxygen atoms of phosphoryl groups, and three water molecules with octahedral geometry. Isothermal titration calorimetry analyses demonstrated that Mg^{2+} ion plays a key role in the enzymatic activity of UGPase by enhancing the binding of UGPase to UTP or UDP-glucose, suggesting that this reaction is catalyzed by an ordered sequential Bi Bi mechanism. Furthermore, the crystal structure explains the specificity for uracil bases. The current structural study combined with functional analyses provides essential information for understanding the reaction mechanism of bacterial UGPases, as well as a platform for the development of novel antibacterial agents.

INTRODUCTION

UDP-glucose pyrophosphorylase (UGPase, EC 2.7.7.9), which is encoded by the *galU* gene, catalyzes the formation of UDP-glucose (UDP-Glc) and pyrophosphate (PPi) from UTP and glucose-1-phosphate (G-1-P). Because it also catalyzes the reverse reaction, it is called glucose-1-phosphate uridylyltransferase and belongs to the nucleotidyltransferase family. UGPase is crucial in carbohydrate metabolism since UDP-Glc is used for the biosynthesis of glycogen and many other carbohydrate derivatives such as glycolipids, glycoproteins and proteoglycans (Flores-Diaz et al., 1997). In various Gram-negative and -positive bacteria, the UGPase activity is required for the biosynthesis of major virulence factors, lipopolysaccharide and capsular polysaccharides (Chang et al., 1996; Genevaux et al., 1999; Mollerach et al., 1998). It was reported that *galU*(-) *Escherichia coli* K-12 produces incomplete lipopolysaccharides and has reduced adhesion activity (Genevaux et al., 1999) and that *galU*(-) *Klebsiella pneumoniae* loses the mucoid colony phenotype and virulence (Chang et al., 1996). In *Streptococcus pneumoniae,* inactivation of UGPase results in defective synthesis of capsular polysaccharides (Mollerach et al., 1998). This enzyme is also involved in the production of galactosyl units for the synthesis of cell wall via the Leloir pathway (Frey, 1996), as *galU*(-) *E. coli* is not able to grow in minimal media supplemented with galactose as the sole carbon source (Genevaux et al., 1999).

UGPases are found in all three kingdoms: eukarya, archaea and bacteria. While bacterial UGPases share high sequence identity, they do not show significant homology with eukaryotic counterparts (Mollerach et al., 1998), suggesting that bacterial UGPases are not evolutionarily related to those in other kingdoms. Therefore, they are considered targets in the development of novel antibacterial agents (Genevaux et al., 1999; Mollerach et al., 1998). Determining the atomic structure of UGPase in complex with substrates and elucidating the catalytic mechanism are of utmost importance for this purpose. The steady-state kinetic studies of G-1-P thymidylyltransferase and G-1-P cytidylyltransferase from *Salmonella enterica*, which also belong to the nucleotidyltransferase family suggested ping pong catalytic mechanism (Lindquist et al., 1993; Lindqvist et al., 1994). According to this mechanism, non-covalent binding of nucleotide tri-phosphate (NTP) to the active site, covalent linkage of nucleotide monophosphate (NMP) to the enzyme, and release of PPi occur sequentially. NMP and G-1-P then condense to form the final product, NDP-Glc (Lindquist et al., 1993; Lindqvist et al., 1994). On the other hand, crystal structure analyses of G-1-P thymidylyltransferases from *Pseudomonas aeruginosa* and *E. coli* proposed ordered sequential Bi Bi mechanism, in which the non-covalent binding of NTP and G-1-P to the enzyme is followed by

Department of Molecular Cell Biology, Samsung Biomedical Research Institute, Sungkyunkwan University School of Medicine, Suwon 440-746, Korea, [1]Department of Studies in Physics, University of Mysore, Manasagangotri, Mysore 570 006, India, [2]Department of Chemistry, College of Natural Sciences, Seoul National University, Seoul 151-742, Korea
*Correspondence: kkim@med.skku.ac.kr

Received September 18, 2009; revised December 18, 2009; accepted December 30, 2009; published online March 15, 2010

Keywords: crystal structure, glucose-1-phosphate uridylyltransferase, isothermal titration calorimetry, reaction mechanism, UDP-glucose pyrophosphorylase

the direct nucleophilic attack of G-1-P on the α-phosphate group of NTP, releasing NDP-Glc and PPi (Blankenfeldt et al., 2000; Zuccotti et al., 2001). The catalytic mechanism of nucleotidyltransferases is known to involve divalent metal cofactors (Kostrewa et al., 2001), mostly Mg^{2+} ion; however, the catalytic role of these ions is still unclear. In the crystal structure of *Corynebacterium glutamicum* G-1-P uridylyltransferase/UDP-Glc complex, two Mg^{2+} ions are coordinated by a phosphoryl oxygen of UDP-Glc, water molecules, and the side chain of aspartic acid (Thoden and Holden, 2007a). However, no Mg^{2+} ions are observed in the crystal structures of G-1-P thymidylyltransferases/TDP-Glc from *P. aeruginosa* and *E. coli* in which the active site residues are linked to substrates directly or via water molecules (Blankenfeldt et al., 2000; Zuccotti et al., 2001).

Structural information of a number of nucleotidyltransferases including UGPase is now available, however, their detailed reaction mechanisms and the role of metal ions are yet to be elucidated in atomic level. Therefore, we determined the crystal structures of UGPase from *Helicobacter pylori* (HpUGPase) in both free and substrate/Mg^{2+}-bound states by the multiple anomalous dispersion (MAD) method, and performed mutational and biochemical experiments based on the information provided by the current crystal structures. While we were preparing this manuscript, the crystal structures of UGPases from *C. glutamicum*, *E. coli*, and *Spingomonas elodea* were published (Aragao et al., 2007; Thoden and Holden, 2007a; 2007b). HpUGPase was similar to those three UGPases in the overall structure, but the structural information combined with mutational and calorimetric studies enabled us to propose the catalytic mechanism of UGPases. The crystal structure of HpUGPase revealed the formation of tetramers and the location of active sites in a deep pocket near the center of molecule. Each substrate or metal binding site is well defined and is expected to serve as a frame for structure-based design of inhibitors. Biochemical studies clearly indicate the Bi Bi mechanism and the crucial role of Mg^{2+} ion in the catalysis.

MATERIALS AND METHODS

Protein preparation and crystallization

HpUGPase was prepared as described previously with minor modifications (Kim et al., 2004). Briefly, *H. pylori galU* gene was subcloned into pET21a vector (Novagen, USA) and the resultant pET21a-*galU* plasmid was transformed into *E. coli* BL21(DE3) competent cells (Novagen, USA). Transformed BL21(DE3) cells were inoculated into Luria-Bertani (LB) broth containing 50 μg/ml ampicillin and cultured at 37°C to an absorbance of 0.5 at 600 nm. After the addition of 0.5 mM IPTG, the cells were grown for additional 4 hours and harvested. The cell pellet resuspended in buffer A (20 mM Tris-HCl pH 7.5, 0.5 M NaCl and 20 mM imidazole) was disrupted by sonication. The clarified lysate was loaded onto a HiTrap chelating column (GE Healthcare, USA) pre-equilibrated with buffer A. Bound UGPase was eluted with a linear gradient of 20 mM - 1.0 M imidazole in buffer A and subsequently applied to a Superdex 200 prep-grade gel filtration column (GE Healthcare, USA) pre-equilibrated with buffer B (20 mM Tris-HCl pH 7.5 and 0.1 M NaCl). The fractions containing UGPase were pooled and used for crystallization. For the preparation of selenomethionine (SeMet) substituted UGPase, *E. coli* methionine auxotroph B834(DE3) (Novagen, USA) harboring the pET21a-*galU* plasmid was grown in M9 medium. SeMet substituted protein was purified as described above for native UGPase, except that 1 mM DTT was added to the buffer as a reducing agent. Crystallization of native and substituted proteins was performed by hanging drop and sitting drop vapor diffusion methods, respectively. Crystals of apo-UGPase were grown in 0.1 M sodium acetate trihydrate (pH 4.6), 2 M ammonium sulfate and 0.1 M guanidine-HCl at 22°C within a week. UDP-Glc/Mg^{2+}-bound holo-UGPase was crystallized in 0.1 M HEPES-Na (pH 7.5), 2% PEG400 and 1.5 M ammonium sulfate containing 10 mM UDP-Glc and 10 mM $MgCl_2$ at 22°C within a month.

Data collection and structure determination

Diffraction data from a flash-frozen UGPase crystal was collected at a resolution of 2.9 Å on a Quantum 4R CCD detector using synchrotron radiation at beamline 38B1 of SPring-8, Japan. MAD data was also collected under the same experimental conditions from a SeMet UGPase crystal with wavelengths of 0.9791 Å (peak), 0.9794 Å (inflection) and 0.9840 Å (remote). Data from a crystal of holo-UGPase was collected at a resolution of 2.3 Å on ADSC Quantum 210 CCD detector using synchrotron radiation at beamline 4A of PAL, Korea. The wavelength of the synchrotron radiation for native crystals was 1.0000 Å. Diffraction data were processed and scaled with the HKL2000 program (Otwinowski and Minor, 1997). The apo-UGPase crystals belonged to the orthorhombic space group $P2_12_12_1$ with unit cell parameters, a = 91.47, b = 98.61, and c = 245.70 Å. The selenium sites and initial phases were calculated using SOLVE and RESOLVE, respectively (Terwilliger, 2001; Terwilliger and Berendzen, 1999). Model building was performed using the program O (Jones et al., 1991). Refinement was performed using the program CNS (Brünger et al., 1998) and the data quality was evaluated using PROCHECK (Laskowski et al., 1993). The final model of UGPase, which was refined at 2.9 Å with R_{work} and R_{free} of 22.5% and 25.4%, respectively, contained four Hp UGPase molecules in an asymmetric unit. The holo-UGPase crystals belonged to the monoclinic space group of C2 in the presence of UDP-Glc and $MgCl_2$ with unit cell parameters, a = 101.44, b = 74.39, c = 167.12 Å, and β = 97.91°. The crystal structure of holo-UGPase was determined by molecular replacement using the program EPMR (Kissinger et al., 1999) with the apo-UGPase structure as a template. The UDP-Glc/Mg^{2+}-bound UGPase was refined at 2.3 Å with R_{work} and R_{free} of 23.0% and 27.6%, respectively. Data collection and refinement statistics are summarized in Table 1. The crystal structure of holo-HpUGPase, which was determined at higher resolution, was used for structural analyses unless specified otherwise. The atomic coordinates and structure factors of apo- and holo-UGPases have been deposited in the Protein Data Bank with accession codes 3JUJ and 3JUK, respectively.

Site-directed mutagenesis

Point mutations were introduced using QuickChange according to the manufacturer's instructions (Stratagene, USA) and were confirmed by DNA sequencing. Mutant proteins were purified in the same way as wild type UGPase. Candidates for the catalytic residue, Arg15, and the substrate-binding residue, Asp130, were replaced with alanine.

Activity assay

The catalytic activity of UGPase was measured by monitoring the decomposition of UDP-Glc. The reaction mixture contained 3 nM UGPase, 20 units of hexokinase/glucose-6-phosphate dehydrogenase (Sigma-Aldrich Co., USA), 2 mM β-NADP, 1 mM UDP-glucose, 10 mM D-glucose, 1 mM pyrophosphate, 10 mM $MgCl_2$, and 0.1 M Tris-HCl (pH 7.5). UGPase converts UDP-Glc and PPi into UTP and G-1-P, and then UTP is consumed in the reduction of β-NADP, which is sequentially catalyzed by hexokinase and glucose-6-phosphate dehydrogenase.

Table 1. Summary of data collection and refinement statistics of UGPases. Values in parentheses refer to the highest resolution shell.

	Apo-UGPase				Holo-UGPase
	Native	Se-Met			Native
		Peak	Inflection	Remote	
Data collection					
Space group	$P2_12_12_1$		$P2_12_12_1$		C2
Unit-cell parameters (Å, °)	a = 91.47	a = 92.11	a = 92.11	a = 92.14	a = 101.44
	b = 98.61	b = 98.72	b = 98.72	b = 98.74	b = 74.39
	c = 245.70	c = 246.28	c = 246.29	c = 246.37	c = 167.12
					β = 97.91
No. of molecules in AU	4				4
Wavelength (Å)	1.0000	0.9791	0.9794	0.9840	1.0000
Resolution range (Å)	50-2.9 (3.0-2.9)		50-2.9 (3.0-2.9)		50-2.3 (2.38-2.30)
Completeness (%)	95.5 (94.0)	99.7(99.9)	99.7(99.9)	99.7(99.9)	98.8 (99.8)
R_{sym} [a] (%)	7.7 (31.0)	8.8 (50.9)	8.3 (49.6)	8.3 (49.2)	10.6 (36.8)
No. of unique reflections	47890	50488	50524	50476	54022
	(4638)	(4979)	(4978)	(4981)	(5092)
Redundancy	4.4	4.8	4.7	4.6	3.1
$\langle I/\sigma(I)\rangle$	19.4 (3.5)	22.9 (3.8)	23.1 (3.9)	23.2 (4.0)	8.1 (3.0)
Refinement					
R_{work} [b] (%)	22.5				23.0
R_{free} (%)	25.4				27.6
No. reflections	45199				45435
No. protein atoms	8688				8397
No. water molecules	95				736
R.m.s. deviations					
Bond lengths (Å)	0.008				0.008
Bond angles (°)	1.59				1.56
Mean *B*-factors (Å^2)					
Protein	57.9				25.8
Main chain	57.0				24.0
Side chain	58.8				26.0
Water	49.3				33.5

[a] $R_{sym}=\Sigma_{hkl}|I-\langle I\rangle|/\Sigma_{hkl}I$

[b] $R_{work}=\Sigma||F_o|-|F_c||/\Sigma|F_o|$

The production of β-NADPH was monitored by measuring the absorbance at 340 nm for 5 min, and the absorbance change per minute was assigned as activity units of UGPase.

Isothermal titration calorimetry analysis

The binding constant of UGPase to the substrate was measured using isothermal titration calorimetry (ITC). Heat change was monitored with the VP-ITC Micro Calorimeter (MicroCal Inc., USA). The sample cell and injection syringe were filled with buffer B containing 10 μM UGPase and 1 mM UDP-Glc, respectively. Heat change upon the addition of substrate solution was monitored and fitted using least-square regression analysis to calculate the dissociation constant (K_d).

RESULTS

Overall structure

The crystal structures of apo- and holo-HpUGPases were determined at 2.9 Å and 2.3 Å resolutions, respectively. HpUGPase forms a homotetramer that can be described as a dimer of dimers with approximate molecular dimensions of 85 Å × 75 Å × 50 Å (Figs. 1A and 1B). The crystal structure of apo-HpUGPase comprises residues 1-273. However, in holo-HpUGPase, residues 71-79 and the C-terminal residue were not modeled due to weak electron density. Each subunit of holo-UGPase contains one UDP-Glc and one Mg^{2+} ion near the active site. Two additional strong electron densities were also assigned to Mg^{2+} because no other metal ion was used in the crystallization experiment. However, being too far from the active site, they do not appear to be of biological relevance. The structures of apo- and holo-UGPases are similar with 1.1 Å root mean square deviations between 264 Cα atoms of protein. Each subunit is composed of eleven α-helices and twelve β-strands, which are arranged into an open twisted central β-sheet surrounded by α-helices on both sides (Fig. 1A).

HpUGPase resembles a Rossman fold, which is a characteristic structural fold found in nucleotidyltransferases and many other nucleotide binding proteins (Figs. 1A and 1C). Although HpUGPase shares a common overall fold with other nucleotidyltransferases (Fig. 1C), its quaternary structure shows distinct subunit packing and symmetry (Figs. 1B and 1D). Subunits A and B are packed by two-fold noncrystallographic symmetry along the axis, which is perpendicular to the α11 helix with a contact area of 2,332 Å^2 (Fig. 1B). On the other hand, subunits

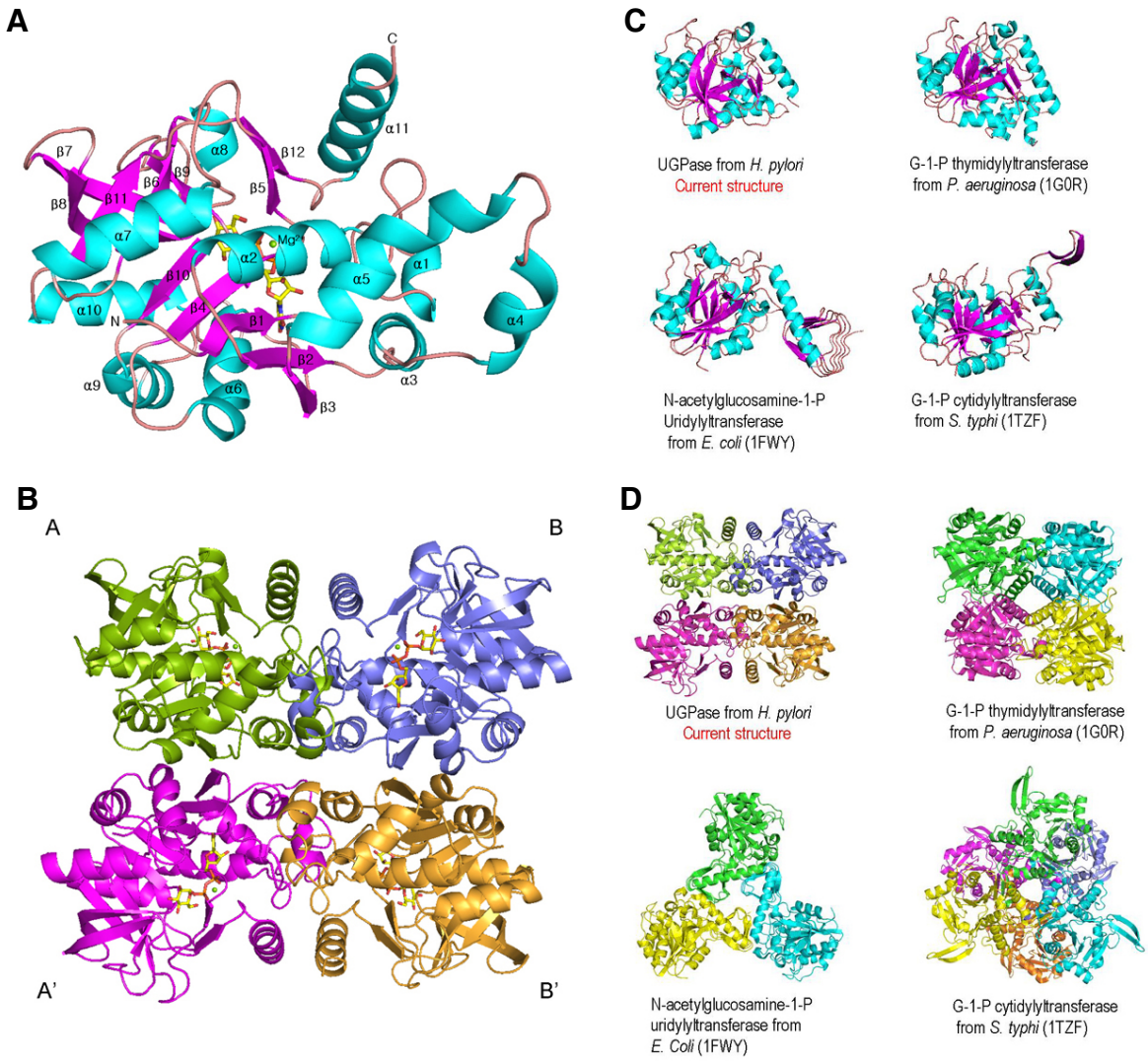

Fig. 1. The overall structure of HpUGPase and its comparison with other nucleotidyltransferases. (A) The subunit structure of *H. pylori* UGPase in complex with UDP-Glc and Mg^{2+} ion is presented in ribbon diagram. α-Helices and β-strands are colored cyan and magenta, respectively, and labeled. UDP-Glc is drawn in yellow stick model. In UDP-Glc, oxygen, nitrogen and phosphate atoms are colored red, blue and orange, respectively. Mg^{2+} ion is shown as a green ball and labeled. (B) Quaternary structure of UGPase is drawn in ribbon diagram. UDP-Glc and Mg^{2+} ion are drawn with the same color schemes as in Fig. 1A. Each subunit is depicted in different colors. (C) Subunit structures of sugar-nucleotidyltransferases are drawn in ribbon diagram. α-Helices and β-strands are colored cyan and magenta, respectively. Their names and PDB IDs are indicated. (D) The ribbon diagrams of the quaternary structures of sugar-nucleotidyltransferases. Each subunit is depicted in different colors.

A and B' or A' and B are related by two-fold noncrystallographic symmetry along the axis, which is parallel to the α11 helix and perpendicular to the symmetry axis of subunits A and B (Fig. 1B). Therefore, the quaternary structure is described as a dimer of dimers. Subunits A and A' are packed with a burial of 1,344 $Å^2$ of the solvent-accessible surface. Accordingly, the subunit pair, A and B or A' and B', has stronger packing interactions than A and A' or B and B' pair. The residues in α1, α3 and α11 helices and α1-α2 loop are mostly involved in the subunit packing between A and B. The binding interface between A and A' is mainly formed by residues in α3 and α5 helices and α5-β3 and β3-α6 loops.

HpUGPase shows high similarity with three other known UGPases in the subunit and quaternary structures (Aragao et al., 2007; Thoden and Holden, 2007a; 2007b). It can be superimposed with *C. glutamicum*, *E. coli*, and *S. elodea* UGPases with root mean square deviations of 2.3 Å, 1.9 Å, and 1.8 Å for 268, 263, and 236 Cα atoms, respectively. The subunits of these UGPases are packed in a similar way to form tetramers.

Active site

The active site of HpUGPase, identified by the positions of UDP-Glc and Mg^{2+} ion, lies in a deep pocket on the central β-sheet surrounded by α-helices (α1, α6, α8 and α10) and neighboring loops connected to those helices (Figs. 1A and 2A). The putative catalytic and substrate binding residues are mainly located on the loops rather than on helices or strands (Fig. 2A). The uridine moiety of UDP-Glc forms hydrogen bonds with Ala10, Gly11, Gln102, and Gly107 residues; the O4 atom of the pyrimidine base interacts with the Nε2 atom of Gln102 and the

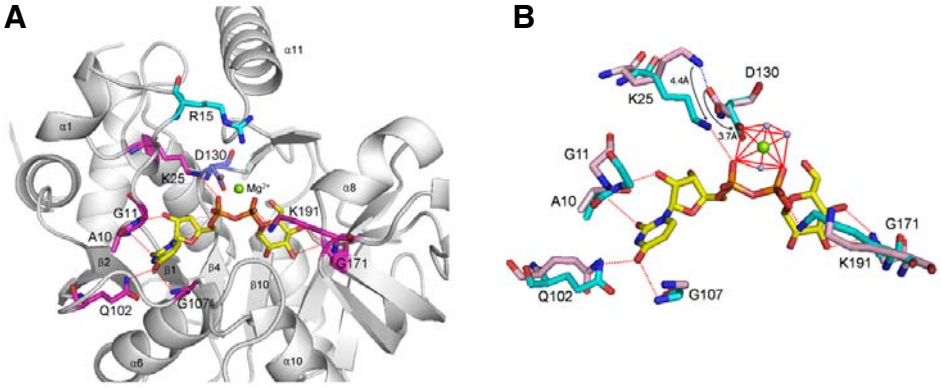

Fig. 2. The active site of HpUGPase. (A) The active site of HpUGPase bound with UGP-Glc and Mg^{2+} ion is drawn as in Fig. 1A. The residues involved in binding to UDP-Glc are depicted in magenta stick mo-dels and labeled. Arg15, a putative catalytic residue, and Asp130, a magnesium binding residue, are colored cyan and blue respectively. (B) The residues in the active site of apo-UGPase (pink) and holo-UGPase (cyan) are compared. Residues are depicted in stick model and labeled. Green and blue balls represent a Mg^{2+} ion and water molecules, respectively. In holo-UGPase, the hydrogen bonds with UDP-Glc are drawn as red dotted lines. A hydrogen bond between Lys25 and Asp130 in apo-UGPase is depicted in a blue dotted line. The black arrows indicate the relocation of Lys25 and Asp130 in apo- and holo-UGPases and the distance changes are in Angstrom units. The octahedral configuration of Mg^{2+} ion coordinated with two phosphoryl oxygens, Asp130 and three water molecules in holo-UGPase is drawn with red lines.

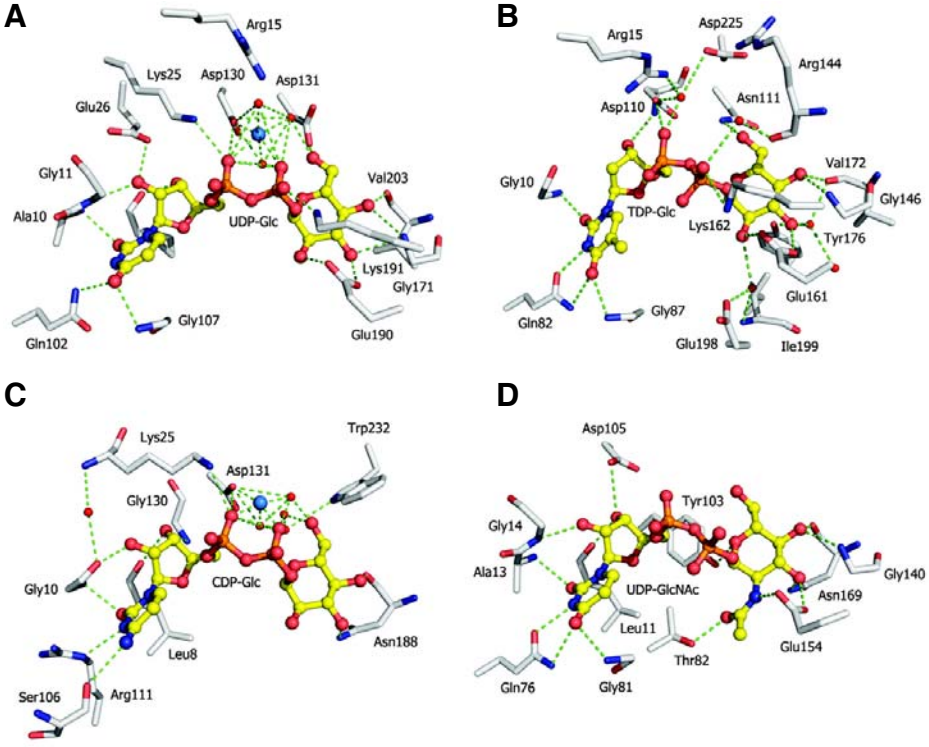

Fig. 3. Active sites of *H. pylori* UGPase and other sugar nucleotidyltransferases. Key residues in the active sites are colored white and the bound substrate is shown in yellow ball and stick model. (A) *H. pylori* UGPase. (B) *P. aeruginosa* G-1-P thymidylyltransferase (1G1L). (C) *S. typhi* G-1-P cytidylyltransferase (1TZF). (D) *E. coli N*-acetylglucosamine-1-P uridylyltransferase (1FWY).

amide nitrogen of Gly107; the O2 atom of the pyrimidine base interacts with the amide nitrogen of Ala10; and the O2' atom of the ribose ring interacts with the amide nitrogen of Gly11 (Fig. 2). The phosphoryl group interacts with Lys25, Lys191 and Mg^{2+} ion, while the O2α atom of α-phosphate and the O2β atom of β-phosphate form hydrogen bonds with Nζ atoms of Lys25 and Lys191, respectively, and form ionic interactions with Mg^{2+} ion (Fig. 2). On the other hand, the glucose moiety interacts with Gly171 via hydrogen bonds with the O3' and O4' atoms of glucose and the amide nitrogen of Gly171 (Fig. 2). The active site residues involved in metal and nucleotide binding are relatively well conserved and their binding modes are similar in other nucleotidyltransferases (Fig. 3).

The binding of UDP-Glc induces local conformational changes near the active site, causing the relocation of Ala10, Gly11, Lys25, Gln102, Gly107, Asp130, Gly171 and Lys191. In particular, Lys25 and Asp130 show remarkable changes since the hydrogen bonds between the Nζ atom of Lys25 and the Oδ1 atom of Asp130 are replaced by new bonds to phosphate and Mg^{2+} ion, respectively (Fig. 2B). These new interactions enhance the binding affinities for substrate and cofactor and neutralize the negative charges of phosphoryl oxygen atoms. Consequently, Mg^{2+} ion is coordinated to the α-phosphate O2α atom, the β-phosphate O1β atom, three water molecules, and the Oδ 1 atom of Asp130 with octahedral geometry (Fig. 2B).

To assess the function of Mg^{2+} ion as a divalent metal cofactor, isothermal titration calorimetry analysis was performed. UGPase formed tight contacts with UDP-Glc with a dissociation

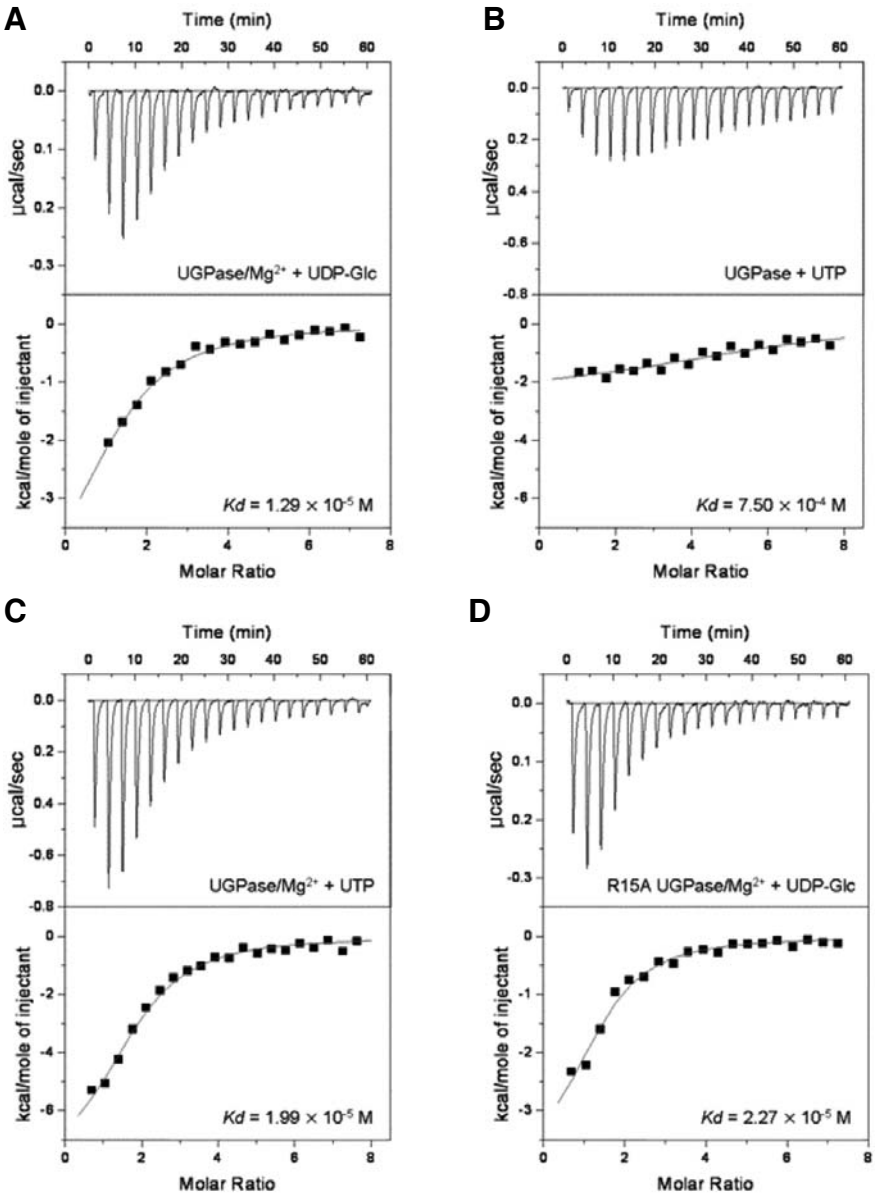

Fig. 4. Isothermal titration calorimetry (ITC) analyses of UGPase with various substrates. The interactions between UGPase/Mg^{2+} and UDP-Glc (A), UGPase and UTP (B), UGPase/Mg^{2+} and UTP (C), and R15A UGPase/Mg^{2+} and UDP-Glc (D) were measured using ITC. The result demonstrates that R15A mutant binds to UDP-Glc with a dissociation constant comparable to that of wild type, and the interaction of UGPase with UDP-Glc or UTP is enhanced by Mg^{2+} ion.

constant (K_d) of 1.29×10^{-5} M in the presence of Mg^{2+} (Fig. 4A); however without Mg^{2+} no interaction was detected (data not shown). Similarly, in UDP-Glc production, Mg^{2+} ion seemed to play an important role in UTP binding because it decreased the dissociation constant of HpUGPase/UTP complex from 7.50×10^{-4} M to 1.99×10^{-5} M (Figs. 4B and 4C). Contrary to the early report concerning the complex formation with UDP-Glc or UTP in the absence of metal ions (Gillett et al., 1971), Mg^{2+} ion seems to be required for the binding of substrate to HpUGPase, a prokaryotic G-1-P uridylyltransferase. Therefore, it is believed that Mg^{2+} is crucial for tethering substrate, particularly, its phosphoryl groups. In consistent with this result, a recent study reported that substrate binding to *S. elodea* G-1-P uridylyltransferase involved Mg^{2+} ion (Aragao et al., 2007).

To study the role of residues in the active site, two residues, Arg15, a putative catalytic residue (Blankenfeldt et al., 2000), and Asp130, a residue involved in substrate binding through Mg^{2+}, were replaced with Ala and the resultant activity changes were measured. R15A and D130A mutants retained only 14% and 7% of the wild type activity, respectively (Fig. 5A), thereby suggesting the important roles of these two residues in the catalysis. Similarly, *P. aeruginosa* G-1-P thymidylyltransferase lost the catalytic activity when its Arg15 equivalent was mutated to Ala (Blankenfeldt et al., 2000). To further investigate the roles of Arg15 and Asp130, the substrate binding affinity of their mutants were analyzed by isothermal titration calorimetry. While R15A mutant strongly bound to UDP-Glc with $K_d = 2.27 \times 10^{-5}$ M (Fig. 4D), which is comparable to that of wild type ($K_d = 1.29 \times 10^{-5}$ M, Fig. 4A), D130A did not interact with UDP-Glc (data not shown). These results indicate that Arg15 contributes to the catalytic activity of UGPase, but Asp130 is involved in binding to substrate.

Reaction mechanism

Both UTP and G-1-P serve as substrates for the production of UDP-Glc. UTP was shown to directly bind to UGPase (Fig. 4C), however, G-1-P did not interact with UGPase as analyzed by ITC (data not shown). These results suggest that UTP binds to

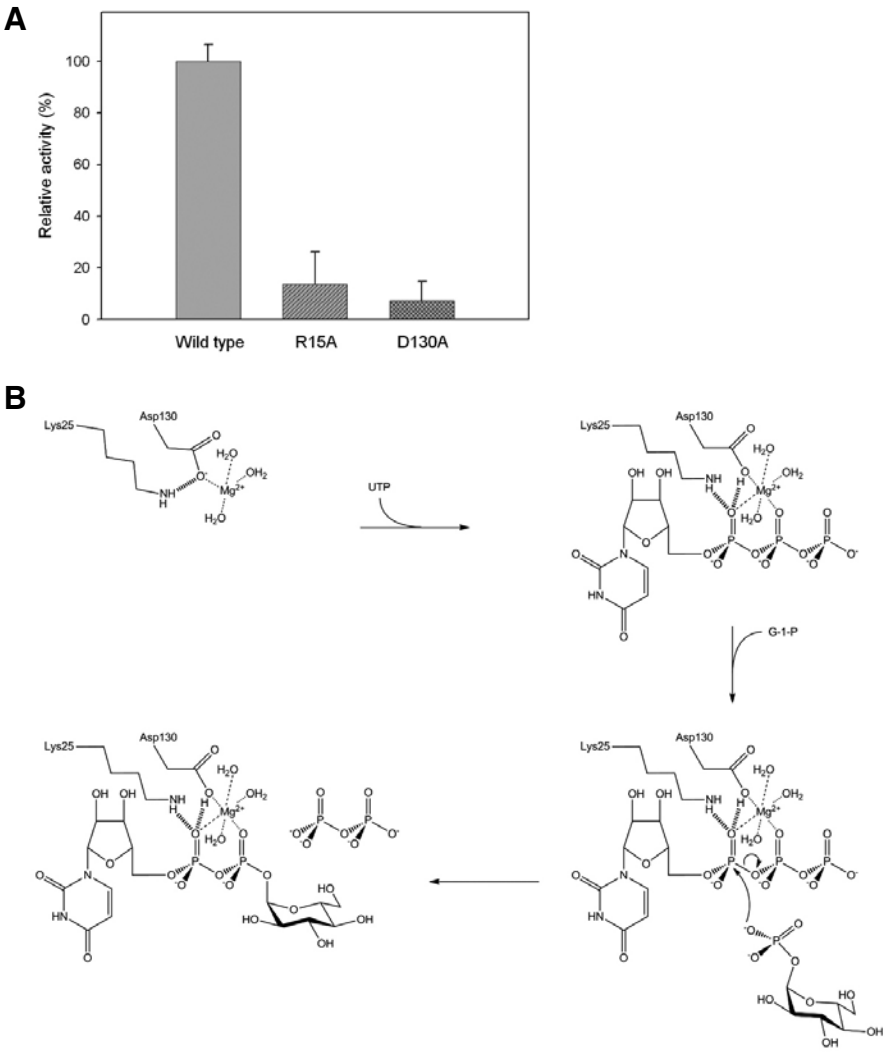

Fig. 5. (A) Catalytic activities of wild type, R15A and D130A UGPases. The relative activities of the mutant UGPases are compared with that of wild-type UGPase. (B) The proposed reaction mechanism of HpUGPase for the conversion of UTP and glucose-1-phosphate to UDP-glucose and pyrophosphate.

UGPase in the presence of Mg^{2+} and then G-1-P binds to the UGPase/UTP complex. Similarly, in the decomposition reaction of UDP-Glc, UDP-Glc would bind to UGPase/Mg^{2+}, followed by the sequential interaction of PPi and UGPase/UDP-Glc/Mg^{2+}, since ITC experiments detected no association between PPi and UGPase/Mg^{2+} (data not shown). Summarizing these results, we propose that Mg^{2+}, UTP and G-1-P bind to UGPase sequentially to form a reaction complex and that PPi is released from the UGPase/UDP-Glc/Mg^{2+} complex after reaction.

Binding specificity for base

To understand the substrate specificities of HpUGPase, its interaction with ATP, GTP, CTP, or TTP was tested by ITC. Interestingly, none of the purine or pyrimidine nucleotides showed significant binding (data not shown). The binding specificities can be explained from the binding mode of HpUGPase and uracil base. Purine bases cannot be accommodated in the base binding cleft of UGPase due to their sizes (Fig. 2A). Pyrimidine bases may approach the base binding site, but they cannot form the tight interactions observed in the HpUGPase/UDP-Glc complex. Thymine binding would be hindered by its extra methyl group, and cytosine could not make specific hydrogen bonds (Fig. 2A).

DISCUSSION

The current study provides a comprehensive understanding of the crystal structure and catalytic mechanism of UDP-Glc pyrophosphorylase (UGPase) from *H. pylori*. Like other bacterial nucleotidyltransferases, HpUGPase exists in a homo-oligomeric structure. Oligomerization of enzymes can be a useful trait for the allosteric control of enzymatic activity, however, the local changes of HpUGPase induced by the substrate binding are not likely to affect the catalytic activity of other subunits. Thus the tetramerization of HpUGPase does not seem to be related to allosterism.

Upon UDP-Glc binding, a hydrogen bond between Lys25 and Asp130 is broken and their side chains move toward the UDP-Glc phosphoryl groups, a hot spot where the condensation and decomposition of the nucleotide-sugar occur. Lys25 forms a hydrogen bond with the O2α atom of UDP-Glc α-phosphate and Asp130 forms an ionic bond with the Mg^{2+} ion. Under these conformational rearrangements, these residues stabilize UDP-Glc via the octahedral coordination of Mg^{2+} ion and the neutralization of the electronegativity of the phosphoryl group. In the reverse reaction, G-1-P and UTP are also expected to be stabilized by the coordination of Mg^{2+} ion and charge neutralization. This geometry could contribute to proper positioning of the phosphoryl group of G-1-P at the α-phosphate

of UTP, thus playing an important role in the nucleophilic attack of G-1-P. In consistent with this, Asp110 of *P. aeruginosa* G-1-P thymidylyltransferase and Asp108 of *E. coli* G-1-P thymidylyltransferase, which structurally overlap with Asp130 of HpUGPase, are also important for the catalytic mechanism (Blankenfeldt et al., 2000; Sivaraman et al., 2002).

The reduced enzyme activity of the R15A mutant implies that Arg15 plays a certain role in catalytic activity of HpUGPase (Fig. 5A). In *P. aeruginosa* G-1-P thymidylyltransferase, its equivalent was also proposed to participate in catalysis (Blankenfeldt et al., 2000). However, the current study cannot provide a clear explanation for the mechanistic role of Arg15, since it is over 6 Å away from the phosphoryl groups of UDP-Glc and is not in direct contact with any other residues. In the crystal structure of holo-UGPase, it is also located away from the hot spot. Therefore, it can be hypothesized that structural rearrangements of the active site are required for Arg15 to approach the phosphate groups and act as a general base during catalysis. Further structural and enzymatic studies are needed to elucidate the reaction mechanism in detail.

Previous studies of bacterial nucleotidyltransferases suggested that Mg^{2+} ion plays an indirect role in catalysis (Kwak et al., 2002) and that the nucleotide triphosphate binding to the active site does not require Mg^{2+} ion (Sivaraman et al., 2002). In our ITC experiments, UTP binding does not require Mg^{2+} ion; however, the presence of Mg^{2+} ion enhances the binding affinity more than 30 times. Furthermore, UDP-Glc cannot interact with UGPase without Mg^{2+}. Therefore, it is certain that Mg^{2+} ion plays a direct and critical role in substrate-tethering, as well as in catalysis. The role of magnesium ion in the catalytic mechanism of UGPase was also revealed from the crystal structure of UGPases from *C. glutamicum* (Thoden and Holden, 2007a). In the presence of Mg^{2+} ion, UTP or UDP-Glc strongly interacts with UGPase, whereas G-1-P or PPi does not bind to UGPase. Therefore, UGPase is thought to form a complex with UTP or UDP-Glc first and then associates with G-1-P or PPi, respectively. These results suggest ordered sequential Bi Bi mechanism as proposed in previous studies (Blankenfeldt et al., 2000; Zuccotti et al., 2001). This reaction mechanism is partially supported by our structural data since UDP-Glc binding to UGPase induced local conformational changes.

Targeting virulence factors has recently emerged as a new antimicrobial development strategy since it has several advantages compared with the conventional methods of targeting *in vitro* viability of bacterial cells (Clatworthy et al., 2007). UGPase is a promising target for this purpose because it plays a critical role in the biosyntheses of most virulence factors; indeed, *galU*(-) cells showed reduced pathogenicity (Chang et al., 1996; Genevaux et al., 1999; Mollerach et al., 1998). In this regard, the current study provides not only a deeper understanding of the molecular mechanism of UGPase but also a platform for the development of novel antibacterial agents.

ACKNOWLEDGMENTS

We thank Dr. Chiwook Park for helpful discussion. We thank the beamline scientists at protein beamlines of Spring8 and PAL for their help during data collection. This work was supported by 21C Frontier Functional Proteomics Program (FPR08B2-270), Ubiquitome Research Program (M10533010001-05N3301-00100) and National Research Laboratory Program (NRL-2006-02287).

REFERENCES

Aragao, D., Fialho, A.M., Marques, A.R., Mitchell, E.P., Sa-Correia, I., and Frazao, C. (2007). The complex of *Sphingomonas elodea* ATCC 31461 glucose-1-phosphate uridylyltransferase with glucose-1-phosphate reveals a novel quaternary structure, unique among nucleoside diphosphate-sugar pyrophosphorylase members. J. Bacteriol. *189*, 4520-4528.

Blankenfeldt, W., Asuncion, M., Lam, J., and Naismith, J. (2000). The structural basis of the catalytic mechanism and regulation of glucose-1-phosphate thymidylyltransferase (RmlA). EMBO J. *19*, 6652-6663.

Brünger, A.T., Adams, P.D., Clore, G.M., DeLano, W.L., Gros, P., Grosse-Kunstleve, R.W., Jiang, J.S., Kuszewski, J., Nilges, M., Pannu, N.S., et al. (1998). Crystallography & NMR system: A new software suite for macromolecular structure determination. Acta Crystallogr. Sect. D Biol. Crystallogr. *54*, 905-921.

Chang, H.Y., Lee, J.H., Deng, W.L., Fu, T.F., and Peng, H.L. (1996). Virulence and outer membrane properties of a *galU* mutant of *Klebsiella pneumoniae* CG43. Microb. Pathog. *20*, 255-261.

Clatworthy, A.E., Pierson, E., and Hung, D.T. (2007). Targeting virulence: a new paradigm for antimicrobial therapy. Nat. Chem. Biol. *3*, 541-548.

Flores-Diaz, M., Alape-Giron, A., Persson, B., Pollesello, P., Moos, M., Eichel-Streiber, C., Thelestam, M., and Florin, I. (1997). Cellular UDP-glucose deficiency caused by a single point mutation in the UDP-glucose pyrophosphorylase gene. J. Biol. Chem. *272*, 23784-23791.

Frey, P.A. (1996). The Leloir pathway: a mechanistic imperative for three enzymes to change the stereochemical configuration of a single carbon in galactose. FASEB J. *10*, 461-470.

Genevaux, P., Bauda, P., DuBow, M.S., and Oudega, B. (1999). Identification of Tn*10* insertions in the *rfaG*, *rfaP*, and *galU* genes involved in lipopolysaccharide core biosynthesis that affect *Escherichia coli* adhesion. Arch. Microbiol. *172*, 1-8.

Gillett, T.A., Levine, S., and Hansen, R.G. (1971). Uridine diphosphate glucose pyrophosphorylase. III. Catalytic mechanism. J. Biol. Chem. *246*, 2551-2554.

Jones, T.A., Zou, J.Y., Cowan, S.W., and Kjeldgaard, M. (1991). Improved methods for building protein models in electron density maps and the location of errors in these models. Acta Crystallogr. A *47*, 110-119.

Kim, H., Wu, C.A., Kim, D.Y., Han, Y.H., Ha, S.C., Kim, C.S., Suh, S.W., and Kim, K.K. (2004). Crystallization and preliminary X-ray crystallographic study of UDP-glucose pyrophosphorylase (UGPase) from *Helicobacter pylori*. Acta Crystallogr. Sect. D Biol.Crystallogr. *60*, 1447-1449.

Kissinger, C.R., Gehlhaar, D.K., and Fogel, D.B. (1999). Rapid automated molecular replacement by evolutionary search. Acta Crystallogr. Sect. D Biol. Crystallogr. *55*, 484-491.

Kostrewa, D., D'Arcy, A., Takacs, B., and Kamber, M. (2001). Crystal structures of *Streptococcus pneumoniae N*-acetylglucosamine-1-phosphate uridyltransferase, GlmU, in apo form at 2.33 Å resolution and in complex with UDP-*N*-acetylglucosamine and Mg^{2+} at 1.96 Å resolution. J. Mol. Biol. *305*, 279-289.

Kwak, B., Zhang, Y., Yun, M., Heath, R.J., Rock, C.O., Jackowski, S., and Park, H. (2002). Structure and mechanism of CTP: phosphocholine cytidylyltransferase (LicC) from *Streptococcus pneumoniae*. J. Biol. Chem. *277*, 4343-4350.

Laskowski, R.A., MacArthur, M.W., Moss, D.S., and Thornton, J.M. (1993). PROCHECK: a program to check the stereochemical quality of protein structures. J. Appl. Crystallogr. *26*, 283-291.

Lindquist, L., Kaiser, R., Reeves, P.R., and Lindberg, A.A. (1993). Purification, characterization and HPLC assay of *Salmonella* glucose-1-phosphate thymidylyl-transferase from the cloned *rfbA* gene. Eur. J. Biochem. *211*, 763-770.

Lindqvist, L., Kaiser, R., Reeves, P.R., and Lindberg, A.A. (1994). Purification, characterization, and high performance liquid chromatography assay of *Salmonella* glucose-1-phosphate cytidylyltransferase from the cloned *rfbF* gene. J. Biol. Chem. *269*, 122-126.

Mollerach, M., Lopez, R., and Garcia, E. (1998). Characterization of the *galU* gene of *Streptococcus pneumoniae* encoding a uridine diphosphoglucose pyrophosphorylase: a gene essential for capsular polysaccharide biosynthesis. J. Exp. Med. *188*, 2047-2056.

Otwinowski, Z., and Minor, W. (1997). Processing of X-ray diffraction data collected in oscillation mode. Methods Enzymol. *276*, 307-326.

Sivaraman, J., Sauvé, V., Matte, A., and Cygler, M. (2002). Crystal structure of *Escherichia coli* glucose-1-phosphate thymidylyltransferase (RffH) complexed with dTTP and Mg^{2+}. J. Biol. Chem. *277*, 44214-44219.

Terwilliger, T.C. (2001). Map-likelihood phasing. Acta Crystallogr. Sect. D Biol. Crystallogr. *57*, 1763-1775.
Terwilliger, T.C., and Berendzen, J. (1999). Automated MAD and MIR structure solution. Acta Crystallogr. Sect. D Biol. Crystallogr. *55*, 849-861.
Thoden, J.B., and Holden, H.M. (2007a). Active site geometry of glucose-1-phosphate uridylyltransferase. Protein Sci. *16*, 1379-1388.
Thoden, J.B., and Holden, H.M. (2007b). The molecular architecture of glucose-1-phosphate uridylyltransferase. Protein Sci. *16*, 432-440.
Zuccotti, S., Zanardi, D., Rosano, C., Sturla, L., Tonetti, M., and Bolognesi, M. (2001). Kinetic and crystallographic analyses support a sequential-ordered Bi Bi catalytic mechanism for *Escherichia coli* glucose-1-phosphate thymidylyltransferase. J. Mol. Biol. *313*, 831-843.